High-temperature photochemistry and BAC-MP4 studies of the reaction between ground-state H atoms and N_2O

Paul Marshall and Arthur Fontijn
Department of Chemical Engineering, Rensselaer Polytechnic Institute, Troy, New York 12180-3590
Carl F. Melius
Sandia National Laboratories, Livermore, California 94550

(Received 31 October 1986; accepted 30 January 1987)

The $H + N_2O$ reaction has been investigated using the high-temperature photochemistry (HTP) technique. $H(1\,^2S)$ atoms were generated by flash photolysis of NH_3 and monitored by time-resolved atomic resonance fluorescence with pulse counting. The bimolecular rate coefficient for H-atom consumption, leading essentially to $N_2 + OH$, from 390 to 1310 K is found to be given by $k_1(T) = 5.5\times10^{-14}\exp(-2380\,\mathrm{K}/T) + 7.3\times10^{-10}\exp(-9690\,\mathrm{K}/T)$ cm^3 molecule^{-1} s^{-1}; the accuracy is assessed as approximately 25% at the 2σ confidence level. Above 750 K, k_1 closely follows the Arrhenius behavior of the second term alone. Distinct curvature is evident below 750 K. k_1 is compared to theoretical BAC-MP4 predictions and good agreement is found for a model involving rearrangement of an HNNO intermediate coupled with tunneling through an Eckart potential barrier, which dominates at the lower temperatures. The branching ratio for the channel leading to NH + NO is discussed in the context of recent thermochemical information and a maximum rate coefficient of $<1\times10^{-9}\exp(-15800\,\mathrm{K}/T)$ cm^3 molecule^{-1} s^{-1} is set for temperatures up to 2000 K.

I. INTRODUCTION

The reaction

$$H(1\,^2S) + N_2O(X\,^1\Sigma_g^+) \rightarrow N_2(X\,^1\Sigma_g^+) + OH(X\,^2\Pi) \quad (1a)$$

is one of the main chain propagating steps in the combustion of H_2/N_2O mixtures[1] and N_2O-supported hydrocarbon flames. Reaction (1a) was investigated by Melville[2,3] in the 1930's and since then there have been several studies, for example using shock tubes,[4–9] flames,[10–13] and a continuously stirred tank reactor (CSTR).[14] This work has been reviewed elsewhere.[1,15,16] Analysis of these observations suffers from the disadvantage that many reactions must be taken into account so that there is considerable uncertainty in individual rate coefficients. There has only been one previous direct study, that of Albers *et al.*,[17] which covered 720 to 1120 K at pressures of 2.6 to 8.0 Torr (1 Torr = 133.3 Pa) and which identified reaction (1a) as the major channel. In the present work the pressure and temperature ranges are extended closer to those relevant to practical combustion. The reaction is of fundamental interest because, despite being highly exothermic, spin allowed, and symmetry allowed,[18–20] it has a large activation barrier.

Because of the importance of obtaining direct measurements of k_1 for the overall reaction

$$H(1\,^2S) + N_2O(X\,^1\Sigma_g^+) \rightarrow \text{products} \quad (1)$$

we have carried out experiments using our high-temperature photochemistry (HTP) reactor, suitable for thermally unstable species such as N_2O, under conditions which isolate reaction (1). The exclusion of secondary reactions simplifies and improves the kinetic analysis.

$k_1(T)$ is found to exhibit significant non-Arrhenius behavior, indicating a possible role of quantum-mechanical tunneling. For this reason a theoretical study of the H/N_2O system is also included.

The alternative minor reaction channel

$$H(1\,^2S) + N_2O(X\,^1\Sigma_g^+) \rightarrow NH(X\,^3\Sigma_g^-) + NO(X\,^2\Pi) \quad (1b)$$

has been suggested as a source of NH[21,22] and as an effective chain termination step in H_2/N_2O flames: subsequent removal of NH by further reactions would terminate the $H + N_2O \rightarrow N_2 + OH/OH + H_2 \rightarrow H_2O + H$ cycle by acting as a sink for chain carriers.[23] The branching ratio k_{1b}/k_1 is discussed.

II. EXPERIMENTAL TECHNIQUE

The general principles of the HTP method[24–27] are similar to conventional flash-photolysis/resonance fluorescence, with the major difference that metal and ceramic construction allows access to a wider temperature range, i.e., 300 to 1800 K. Details of the apparatus have been described recently.[24,25] An important feature of the HTP reactor is the cooled inlet.[24–27] This permits thermally unstable gases such as NH_3 and N_2O to be injected into the reactor and to be heated by mixing with the Ar bath gas, a procedure which minimizes heterogeneous decomposition. Because the diffusion times to the sides of the reaction tube are relatively long, the reaction zone (defined by the intersection of the cones of light from the flash lamp and the microwave-powered resonance lamp)[24] is essentially wall-less.

A small fraction of N_2O was mixed with a slow flow of Ar bath gas along a heated mullite reaction tube and H atoms were generated photolytically from NH_3. The reduction of [H] through reaction and diffusion was monitored by time-resolved resonance fluorescence at $\lambda = 121.6$ nm

 0021-9606/87/105540-10$02.10

$[H(2\,^2P) \rightarrow H(1\,^2S)]$ with pulse counting and signal averaging. In order to vary the photolysis conditions flash energies of 20 to 200 J were employed, and both Suprasil quartz and magnesium fluoride were used as the flash lamp window material.[24] A dry air filter[24] was placed in front of the photomultiplier tube to eliminate any N-atom or O-atom radiation. Checks showed that photolysis of N_2O alone gave insignificant signals, as expected in view of the use of this filter and the small absorption cross section of N_2O.[28]

The gases used in the reactor, all from the liquid, were Linde 99.998% Ar, Linde "Anhydrous Grade" 99.99% NH_3 and Matheson "Semiconductor Grade" 99.998% NH_3 as the source of H atoms, and Linde "Atomic Absorption Grade" 99.0% N_2O ($O_2 < 0.2\%$ by mass spectrometric analysis) and Matheson "Ultra High Purity" 99.99% N_2O. Results from the different grades of NH_3 and N_2O were the same.

The reaction was studied under pseudo-first-order conditions, $[H] \ll [N_2O]$, $[NH_3]$. Following its pulsed generation atomic H was lost from the reaction zone primarily by diffusion (k_D) and by reaction with NH_3 (k_{NH3}) and N_2O (k_1):

$$\frac{-d[H]}{dt} = k_D[H] + k_{NH3}[NH_3][H] + k_1[N_2O][H] = k_{ps1}[H], \quad (2)$$

where k_{ps1} is the pseudo-first-order decay coefficient for [H] as a function of time t.[24] The fluorescence intensity I_t is given by

$$I_t = I_0 \exp(-k_{ps1}\, t) + B, \quad (3)$$

where B represents the steady background due to scattered light from the resonance lamp. Observed I_t data were analyzed on a microcomputer using a three-parameter nonlinear weighted least-squares routine.[29] This program is an improvement over that described earlier[24] as B does not need to be determined from I_t at long times. Equation (2) indicates that, provided the total pressure and $[NH_3]$ and thus k_D and k_{NH3} are kept constant, plots of k_{ps1} vs $[N_2O]$ should be linear with slope k_1. An upper temperature limit of 1310 K was set by the consumption of H by NH_3 alone, a process which becomes fast at this temperature.[24] Errors were estimated and propagated as described before.[24]

III. EXPERIMENTAL RESULTS

The values of k_1 obtained, together with the experimental conditions, are listed in Table I. P represents the total pressure and $[M]$ the total concentration, which is the more significant quantity. Also given are $\bar{v}$ the average linear gas velocity, l the distance of the inlet from the reaction zone, and F the energy dissipated in the flash lamp. Inspection of Table I reveals that, within the scatter of k_1, there is no consistent variation of k_1 with $[M]$ which was changed by a factor of 15. k_1 is also independent of the purely experimental parameters $\bar{v}$, l, and F which were varied by factors of 15, 23, and 9, respectively, confirming that significant decomposition of N_2O was avoided, thermal equilibrium was achieved and gas flows were well mixed. Significant secondary reactions of H are ruled out since (i) k_1 does not depend on $[M]$, eliminating the possibility of recombination reactions with O or trace impurities, and (ii) k_1 is independent from the flash intensity, which shows that the influence of photolysis and reaction products is negligible.

At each temperature k_{ps1} was measured as a function of $[N_2O]$ typically at six concentrations from 0 to $[N_2O]_{max}$ (see Table I) to find k_1, cf. Eq. (2). Forty-four measurements of k_1 were made from 390 to 1310 K, covering a range of rate coefficients of 1×10^{-16} to 6×10^{-13} cm^3 molecule^{-1} s^{-1}. These are plotted in Arrhenius form as Fig. 1. The data for $T > 750$ K may be fitted to the simple expression $A \exp(-B/T)$,

$$k_1(T) = 7.3\times10^{-10} \times \exp(-9500 \pm 430\ \text{K}/T)\ \text{cm}^3\ \text{molecule}^{-1}\ \text{s}^{-1}, \quad (4)$$

where the error in $\ln A$ is ± 0.44 and the limits represent $\pm 1\sigma$ in the individual parameters.

Figure 1 shows that another expression needs to be derived to encompass the whole experimental temperature range. A fit to the form $A(T/\text{K})^n \exp(-B/T)$ yields $A = 1.8\times10^{-54}$ cm^3 molecule^{-1} s^{-1}, $n = 12.9$ and $B = -4100$ K. These parameters are unreasonable for a transition state-type expression describing a single reaction pathway and the expression extrapolates with excessive curvature. A fit to the form $A \exp(-B/T) + C \exp(-D/T)$ was carried out to give

$$k_1(T) = 8.4\times10^{-14} \exp(-2580\ \text{K}/T) + 2.6\times10^{-9} \times \exp(-10\,980\ \text{K}/T)\text{cm}^3\ \text{molecule}^{-1}\ \text{s}^{-1}. \quad (5)$$

A disadvantage to fitting rate coefficient data to many-parameter expressions is that uncertainties in individual terms can become large and the physical significance is lost: Here there is particular uncertainty associated with the large value of the preexponential factor C, which therefore may not be meaningful. Consequently, we favor constraining this parameter to agree with the value from Eq. (4), yielding

$$k_1(T) = 5.5\times10^{-14} \exp(-2380\ \text{K}/T) + 7.3\times10^{-10} \times \exp(-9690\ \text{K}/T)\text{cm}^3\ \text{molecule}^{-1}\ \text{s}^{-1}, \quad (6)$$

which is shown in Fig. 1. The variances of the parameters ($\sigma_A^2 = 3.1\times10^{-28}$, $\sigma_B^2 = 2.8\times10^4$, $\sigma_D^2 = 5.6\times10^3$) and covariances ($\sigma_{AB} = 2.9\times10^{-12}$, $\sigma_{AD} = 7.0\times10^{-13}$, $\sigma_{BD} = 6.3\times10^3$), which reflect coupling between the three dependent parameters A, B, and D were used[30,31] to estimate 2σ statistical confidence limits for $k_1(T)$. These are 26% at $T = 390$ K, falling to about 9% to 12% for $T > 500$ K. We believe these precision figures also account for systematic errors, as suggested by the close agreement with other experiments (see below). Nevertheless we allow for possible systematic errors of 15%. This leads to an accuracy assessment of 30% at $T = 390$ K, narrowing to approximately 19% for $T > 500$ K. Equation (6) gives values of k_1 very close to those from Eq. (5), and also Eq. (4) for $T > 750$ K, indicating that relatively wide variations in parameters lead to only small changes in k_1. This illustrates that it is important to compare $k(T)$ values from published recommendations rather than the expressions themselves.

TABLE I. Summary of rate coefficient measurements on $H + N_2O$.

$T \pm \sigma_T$ (K)	P (Torr)[a]	$[M]$ (10^{18} cm^{-3})	$[N_2O]_{max}$ (10^{15} cm^{-3})	$[NH_3]$ (10^{15} cm^{-3})	$\bar{v}$ (cm s^{-1})	l (cm)	F (J)[b]	$k \pm \sigma_k$ (cm^3 molecule^{-1} s^{-1})
385 ± 8	80	2.0	64	7.2[e]	3.3	17	200	1.2 ± 0.5 (−16)[c]
388 ± 8	430	11	57	4.2[e]	3.0	17	50	1.0 ± 1.2 (−16)
413 ± 8	110	2.7	58	4.1	7.8	17	50	1.55 ± 0.08(−16)
439 ± 9	320	7.1	70	3.9	4.6	46	22	2.8 ± 0.3 (−16)
467 ± 9	130	2.6	74	3.9	7.4	46	50	2.8 ± 0.4 (−16)
501 ± 10	190	3.7	65	4.2	8.9	46	140	5.5 ± 0.3 (−16)
513 ± 10	180	3.4	67	3.3	10	46	50	4.1 ± 0.3 (−16)
522 ± 10	180	3.2	66[d]	5.9	8.9	9.5	50*M*	5.8 ± 0.3 (−16)
539 ± 11	300	5.4	45	1.0	6.2	46	22	8.3 ± 0.3 (−16)
545 ± 11	200	3.6	47	7.1	9.1	46	140	8.1 ± 0.3 (−16)
563 ± 11	53	0.91	51	3.1	12	17	50	5.8 ± 1.7 (−16)
565 ± 11	250	4.4	46	4.4	4.7	17	50	9.4 ± 0.5 (−16)
611 ± 12	200	3.1	49[d]	3.6	9.4	9.5	50*M*	1.24 ± 0.06(−15)
643 ± 13	110	1.7	59[d]	2.7	20	10	50	1.2 ± 0.2 (−15)
679 ± 14	270	3.9	74[d]	3.2	5.2	10	50	1.93 ± 0.07(−15)
690 ± 14	420	5.9	51	3.6	8.2	46	140	2.8 ± 0.1 (−15)
697 ± 14	110	1.5	38[d]	2.5	21	17	50	2.7 ± 0.1 (−15)
714 ± 14	240	3.2	55[d]	3.8	9.0	8	50*M*	2.8 ± 0.3 (−15)
716 ± 14	110	1.5	42[d]	3.6	13	10	50	3.0 ± 0.1 (−15)
772 ± 15	250	3.2	37[d]	2.4	12	10	50	4.3 ± 0.2 (−15)
790 ± 16	240	2.9	69[d]	3.8	10	8	40*M*	4.6 ± 0.2 (−15)
797 ± 16	130	1.6	30[d]	2.2	24	17	50	5.9 ± 0.3 (−15)
846 ± 17	150	1.8	35[d]	2.3	18	13	50*M*	6.7 ± 0.5 (−15)
847 ± 17	110	1.3	24[d]	3.0	15	10	50	1.1 ± 0.1 (−14)
867 ± 17	270	3.0	24[d]	2.7	6.6	10	50	1.16 ± 0.06(−14)
877 ± 18	110	1.2	13	2.0	17	17	22	2.2 ± 0.1 (−14)
901 ± 18	150	1.6	37[d]	2.1	19	4.5	50*M*	1.26 ± 0.08(−14)
907 ± 18	320	3.4	50[d]	2.1	9.1	4.5	50*M*	1.5 ± 0.1 (−14)
916 ± 18	130	1.4	14[d]	1.2	28	17	50	2.7 ± 0.1 (−14)
938 ± 19	110	1.1	15[d]	1.8	16	10	50	3.3 ± 0.1 (−14)
959 ± 19	160	1.6	25[d]	1.0	20	4.5	50*M*	1.8 ± 0.5 (−14)
963 ± 19	200	2.0	8.1	1.9	17	8.5	50	3.6 ± 0.2 (−14)
973 ± 19	110	1.1	9.7[d]	1.7	18	17	50	5.2 ± 0.3 (−14)
998 ± 20	300	2.9	13	2.2	11	3	200	3.9 ± 0.1 (−14)
1010 ± 20	92	0.89	12[d]	0.71	25	4.5	50*M*	4.0 ± 0.5 (−14)
1015 ± 20	200	1.9	5.1	1.3	18	8.5	50	5.7 ± 0.4 (−14)
1016 ± 20	200	1.9	7.4[d]	0.42	18	4.5	50	1.06 ± 0.07(−13)
1073 ± 21	230	2.0	4.8	3.0[e]	16	3	50	9.4 ± 0.5 (−14)
1126 ± 23	190	1.6	2.2	0.5	21	3	50	1.5 ± 0.1 (−13)
1159 ± 23	310	2.6	1.6[d]	0.96[e]	13	6	22	2.6 ± 0.3 (−13)
1184 ± 24	92	0.75	2.8	1.1[e]	44	3	50	2.6 ± 0.4 (−13)
1211 ± 24	200	1.6	1.2	0.44[e]	20	2	50	3.4 ± 0.5 (−13)
1302 ± 26	150	1.1	0.2	0.23[e]	34	3	50	5.8 ± 2.4 (−13)
1314 ± 26	150	1.1	3.9	1.5[e]	30	3	50	3.8 ± 1.3 (−13)

[a] 1 Torr = 133.3 Pa.
[b] The suffix "*M*" indicates that photolysis was through a flat magnesium fluoride window. Otherwise a Suprasil quartz $f/1.5$ lens was used.
[c] Should be read as $(1.2 \pm 0.5) \times 10^{-16}$.
[d] Linde 99.0% N_2O employed, rather than Matheson 99.99% N_2O as in the other experiments.
[e] Matheson 99.998% NH_3 employed. The other experiments were with Linde 99.99% NH_3.

IV. COMPARISON WITH EARLIER MEASUREMENTS

The only other direct measurements of k_1 are those of Albers *et al.*[17] over the temperature range 720 to 1120 K (see Fig. 1 and Table II). They used a discharge/fast-flow reactor with ESR detection of H atoms, a procedure which required stoichiometric corrections to the observed k_1 values from 0% to 50%. Their results nonetheless show excellent agreement with the present work where secondary reactions do not have to be taken into account. They[17] obtained data at $[M]$ from $(3 \text{ to } 10) \times 10^{16}$ cm^{-3}, an order of magnitude smaller than in the present work, which thus extends the range of the observed $[M]$ independence.

Table II summarizes the results of other studies of reaction (1). Since reaction (1b) is a minor contributor (see later) a number of determinations nominally of k_{1a} alone are included. These data are shown in Fig. 2 and it may be seen that, despite the wide variation in the quoted Arrhenius parameters (A from 5.2×10^{-11} to 3.0×10^{-9} cm^3 molecule^{-1} s^{-1} and E_a/R from 6000 to 13 100 K), there is general agreement between the flame and shock tube data for k_1 and an extrapolation of the present work [Eq. (6)]. However, agreement between the activation energies for these data is less satisfactory. This is not surprising in view of the

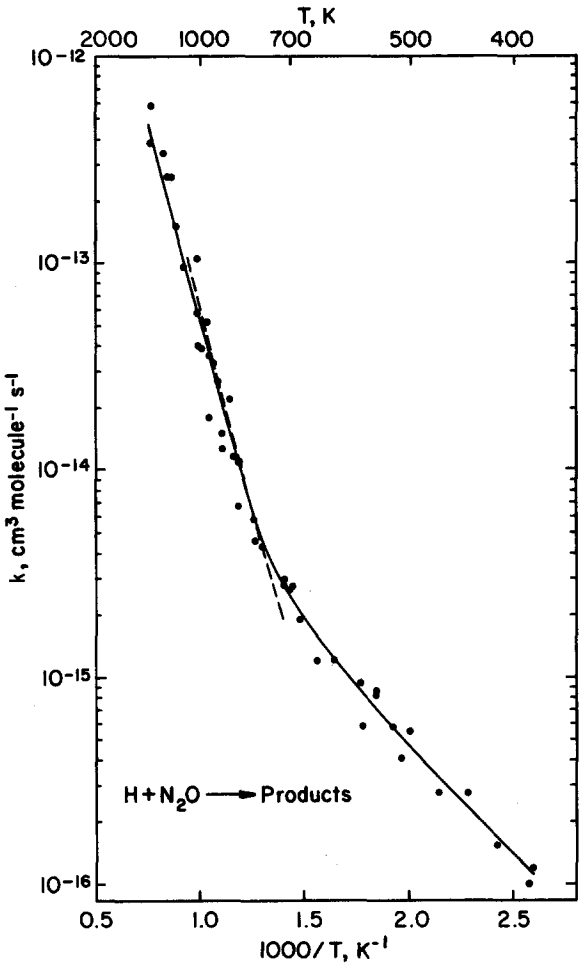

FIG. 1. Plot of the rate coefficients obtained for the reaction $H + N_2O \rightarrow$products. (●) Present work, HTP. (—) Fit to present work. (- - -) Results of Albers *et al.* (Ref. 17), discharge/fast flow reactor.

fact that all these determinations of k_1 are dependent on the kinetic scheme and rate parameters assumed. The widely used recommendation of Baulch *et al.*,[15] $k_1(T) = 1.3\times10^{-10}\exp(-7600\ \text{K}/T)$ $\text{cm}^3\ \text{molecule}^{-1}\ \text{s}^{-1}$ (error limits ± 50%), appears quite different from Eq. (6). Nonetheless the difference between Eq. (6) and the Baulch *et al.*[15] recommendation is − 15% at 1300 K and 45% at 800 K, well within the combined uncertainties.

V. THEORETICAL CALCULATION OF THERMOCHEMICAL PARAMETERS

The geometries, frequencies, and enthalpies for the transition state (TS) structures as well as reactants, products, and stable intermediates have been calculated using the BAC-MP4 method.[35–37] The procedure involves several steps. First the geometries of the reactants, products, and stable intermediates were optimized using the Hartree–Fock method. For the TS structures, a stationary point on the potential energy surface corresponding to one imaginary frequency (the saddle point) was found using the same method. Hartree–Fock harmonic oscillator frequencies, determined from the second derivative matrix, were scaled downward by 12%. These frequencies are listed in Table III. Next, enthalpies for each of the molecular species and TS structures were determined using the Møller–Plesset fourth-order perturbation theory (MP4), which includes electron correlation effects. Finally, bondwise additive corrections (BAC) and spin contamination corrections were included to correct for the finite basis set, for the finite electron correlation and for the unrestricted Hartree–Fock wave function used in the MP4 step.

The resulting heats of formation and free energies are given in Table IV. The enthalpies given in Table IV differ slightly from those of Ref. 35 because of changes in estimating the error due to spin contamination. The spin contamination in the HNNO molecule and the corresponding transition states is large [$S(S+1) > 1.0$ compared to the correct value of $S(S+1) = 0.75$ for doublet states]. This leads to large spin corrections of 20 to 60 kJ mol^{-1}. Consequently, there are larger estimated errors (about 20 kJ mol^{-1}) compared to the 10 kJ mol^{-1} estimated for the reactants and

TABLE II. Previous rate coefficient measurements on $H + N_2O \rightarrow$products, expressed in the form $k_1(T) = A\exp(-B/T)$.

A ($\text{cm}^3\ \text{molecule}^{-1}\ \text{s}^{-1}$)	B (K)	T range (K)	Comments
3.7×10^{-10}	8 710	720–1120	Ref. 17 discharge/ fast-flow reactor
5.2×10^{-11}	6 070	1210–1760	Ref. 10 flame study as recalculated in Ref. 16.
1.0×10^{-10}	6 590	1000–1600	Ref. 13 flame study
6.6×10^{-11}	6 000	1700–2600	Ref. 6 shock tube
3.0×10^{-9}	13 600	2000–2850	Ref. 4 shock tube
1.5×10^{-9}	11 100	1600–3000	Ref. 5 shock tube
2.5×10^{-10}	7 550	1450–2200	Ref. 8 shock tube
6.4×10^{-11}	8 510	1470–2710	Ref. 9 discharge flow/shock tube
3.5×10^{-10}	13 100	1600–2100	Ref. 32 shock tube
7.1×10^{-14}	···	900	Ref. 12 flame study
4.8×10^{-13}	···	1360	Ref. 11 flame study
4.3×10^{-15}	···	770	Ref. 14 CSTR
1×10^{-17}	···	400	Ref. 33 upper limit, CSTR
2×10^{-17}	···	423	Ref. 34 order of magnitude estimate, CSTR

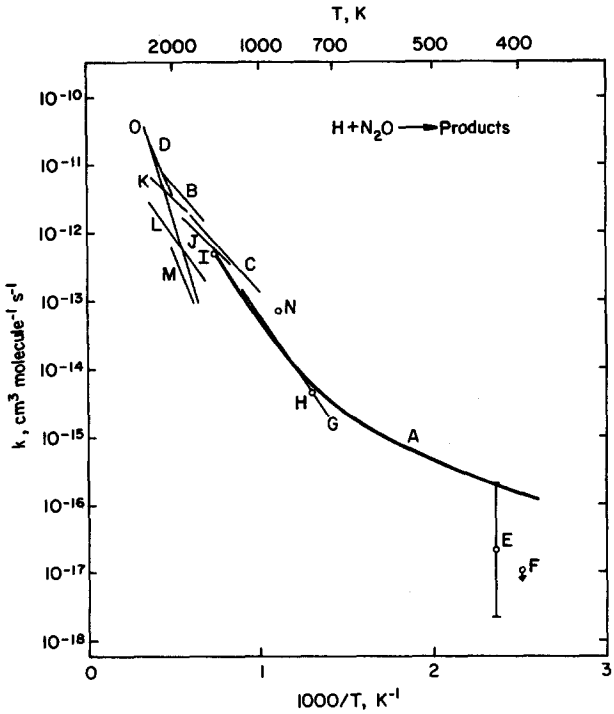

FIG. 2. Comparison of various experimental determinations of $k_1(T)$ for the reaction $H + N_2O \rightarrow$ products. A: This work (heavy line), B: Hidaka *et al.* (Ref. 8), C: Balakhnine *et al.* (Ref. 13), D: Dean *et al.* (Ref. 4), E: Schiavello *et al.* (Ref. 34), F: Johnson and Simic (Ref. 33) (upper limit), G: Albers *et al.* (Ref. 17). H: Baldwin *et al.* (Ref. 14), I: Dixon-Lewis *et al.* (Ref. 11), J: Fenimore and Jones (Ref. 10), K: Henrici and Bauer (Ref. 6), L: Glass and Quy (Ref. 9), M: Nip (Ref. 32), N: Dixon-Lewis *et al.* (Ref. 12), and O: Dean *et al.* (Ref. 5).

products. However, this accuracy is sufficient to distinguish between competing pathways for the reaction and to make estimates of the reaction rate coefficients (which, as will be seen, are supported by the experimental data). These uncertainties in energy barriers do not apply to calculated preexponential factors which depend on geometries and vibrational frequencies. The resulting reaction coordinate diagram is shown in Fig. 3.

BAC-MP4 calculations have been made for three states of the HNNO intermediate, *cis*-$^2A''$, *cis*-$^2A'$, and *trans*-$^2A'$, yielding $\Delta H^\circ_{f,300\,K}$, of 313, 234, and 250 kJ mol^{-1}, respectively. We concentrate on the $^2A'$ surface for reaction (1a), because reactants and products correlate along a $^2A'$ surface on the basis of C_s symmetry in the "least-symmetrical complex" and the weak spin-orbit coupling approximation.[18–20] Information for the *cis* form is used in kinetic calculations because it is the most stable isomer and also is structurally more suited to a 1,3-hydrogen shift. Only this form is shown in Fig. 3.

TABLE III. BAC-MP4 vibrational frequencies for the transition states and intermediates shown in Fig. 3.

Species	Frequencies (cm^{-1})
A: $N_2O + H \rightarrow N_2 + OH$[a]	352, 504, 639, 1057, 1640, 1559*i*
B: $H + N_2O \rightarrow HNNO$[a]	375, 590,[b,c] 759, 1174, 1829, 1287*i*
C: *cis* $^2A'$–HNNO	312, 843,[b,d] 1042, 1294, 1463, 3210
D: $HNNO \rightarrow N_2 + OH$[a]	481, 807, 958, 1280, 1767, 2427*i*

[a] Tabulated values are for the transition state of this reaction.
[b] This vibrational mode is replaced by a hindered internal rotor about the N–N bond.
[c] Barrier height is 335 kJ mol^{-1}; symmetry number is 1.
[d] Barrier height is 111 kJ mol^{-1}; symmetry number is 2.

VI. DISCUSSION

An Arrhenius plot of the present data (Fig. 1) exhibits significant curvature. To interpret this temperature dependence as well as to predict the possible reaction products, we apply transition state theory (TST) with tunneling.

A. The $H + N_2O \rightarrow N_2 + OH$ channel (1a)

This reaction is highly exothermic, $\Delta H^\circ_{298\,K} = -261$ kJ mol^{-1},[38] yet the observed high temperature enthalpy barrier for the reaction [Eqs. (4) and (6)] is about 80 kJ mol^{-1}. As can be seen from Fig. 3 both a "direct" pathway and an "indirect" one are consistent with this large energy barrier. The direct pathway is the addition of an H atom to the oxygen end of N_2O to form the unstable NNOH intermediate, which immediately dissociates to N_2 and OH. The calculated enthalpy barrier relative to the reactants for this direct process is 79 kJ mol^{-1} at 300 K (Table IV). Within the limits of the Hartree–Fock calculations the NNOH structure is unbound, corresponding not to a well but instead a plateau of the potential energy surface. In order to derive the ΔH°_f(NNOH) shown in Fig. 3 the N–O distance was constrained to be 1.4 Å (1 Å = 10^{-10} m), equal to that in H_3NOH. We stress that the direct mechanism is distinct from simple abstraction. Rather than initial H attack at the

TABLE IV. Calculated thermochemical quantities using the BAC-MP4 method. (Energies in kJ mol^{-1}.)

	ΔH°_f		ΔG°_f				
Species	0	300 K	300 K	600 K	1000 K	1500 K	2000 K
H	216	218	203	187	165	136	106
N_2O	85	82	104	127	156	192	227
A: $N_2O + H \rightarrow N_2 + OH$[a]	384	378	409	440	481	531	581
B: $H + N_2O \rightarrow HNNO$[a]	316	311	342	374	417	470	522
C: *cis* $^2A'$–HNNO	240	234	264	295	336	387	436
D: $HNNO \rightarrow N_2 + OH$[a]	371	365	396	429	474	528	583

[a] Tabulated values are for the transition state of this reaction.

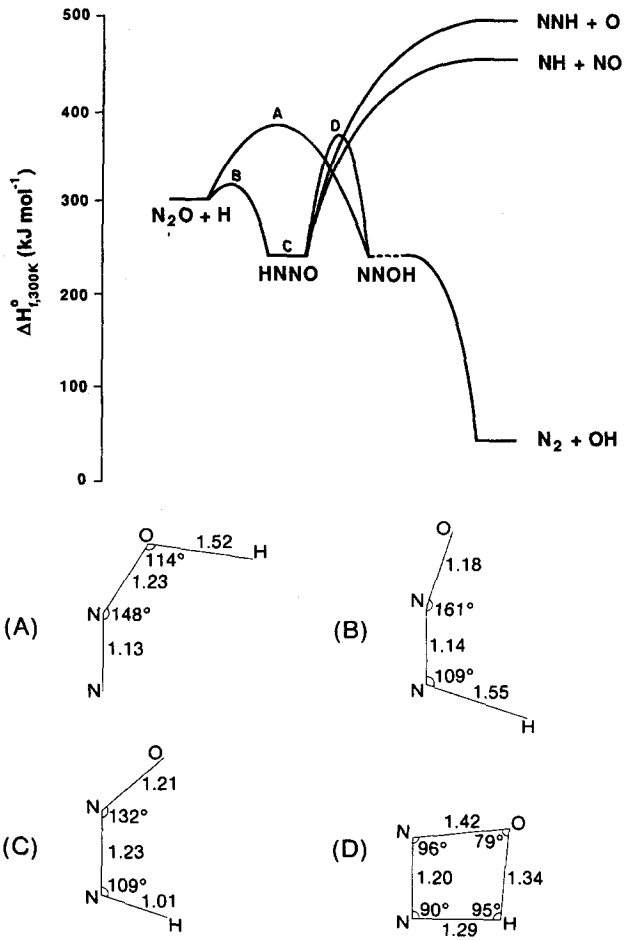

FIG. 3. (a) Enthalpies of formation at 300 K for species and transition states for the reaction $H + N_2O \rightarrow$ products calculated by the BAC-MP4 theoretical method, showing two pathways leading to $N_2 + OH$. The direct route passes through A while the 1,3-hydrogen shift route passes through B, C, and D. (b) Scale drawings of the planar intermediate configurations shown in (a). All distances in units of 10^{-10} m.

O atom with simultaneous weakening of the N–O bond, which would lead to a large preexponential factor because of the loose TS, the H atom first adds to the multiple N–O bond followed by rearrangement to NNOH which falls apart. Evidence for this mechanism is that the length of the N–O bond in N_2O is 1.18 Å while the N–O distance in the direct TS has only increased to 1.23 Å, by contrast to the 1.4 Å typical of a single bond.

The alternative indirect mechanism involves addition of H to the nitrogen end of N_2O to form the stable HNNO species followed by a 1,3-hydrogen shift to make the unstable NNOH intermediate; the addition process has an enthalpy barrier of 11 kJ mol^{-1} at 300 K while the 1,3-hydrogen shift has an overall enthalpy barrier of 65 kJ mol^{-1} at 300 K, both barriers calculated relative to $N_2O + H$. The reaction coordinate for this indirect or 1,3-hydrogen shift mechanism corresponds to Golden's "Scheme I",[39] comprising an intermediate bound complex where the barrier to decomposition back to reactants is lower than the one inhibiting passage to final products, as indicated in Fig. 3. The overall rate coefficient in such cases is pressure independent and is given by the product of the equilibrium constant for formation of the complex and the unimolecular decay rate to final products.[39] We mention in passing that the total rate for such a system $A + B \rightleftharpoons C \rightarrow D$ is independent of $\Delta G^\circ_f(C)$, since the contribution to the equilibrium constant is exactly balanced by the effect on the rate coefficient for $C \rightarrow D$, according to simple TST.

We have calculated k_{1a} according to both the direct and indirect mechanisms (see Table V). Rate coefficients were calculated with the simple TST formula $k = (k_B T/h) \times \exp(-\Delta G^{\neq}/RT)$, where $\Delta G^{\neq}$ is the free energy of formation of the TS from reactants, relative to the appropriate standard states. Effects of tunneling have been allowed for by fitting an Eckart potential[40,41] to the enthalpy surface at 300 K, using values of ω^*, the "vibrational" frequency along the reaction coordinate for the TS.[41] BAC-MP4 gave $\omega^* = 1559$ and 2427 cm^{-1} for the direct and indirect or hydrogen shift mechanisms, respectively. As in our study of $H + NH_3$,[24] some uncertainty is introduced into the tunneling correction both from ω^* and from fitting the reaction coordinate to a one-dimensional potential.[41] The BAC-MP4 method tends to overestimate the imaginary frequency derived from the Hartree–Fock calculations because of the large MP4 and BAC corrections to the barrier height. However, for the 1,3-hydrogen shift, the large imaginary frequency results from the large barrier height with respect to the bottom of the HNNO potential well (131 kJ mol^{-1}). In this case the BAC correction factors tend to cancel. Thus, the large value of ω^* for the 1,3-hydrogen shift is probably reasonable.

Table V indicates that the two mechanisms including tunneling effects both yield rate coefficients which are fairly close to experiment at high temperatures ($T > 1000$ K).

TABLE V. Comparison of observed rate coefficients for $H + N_2O \rightarrow OH + N_2$ with theoretical values calculated from BAC-MP4 data. (All rates in cm^3 molecule^{-1} s^{-1}.)

T (K)	1,3 H shift	1,3 H shift and tunnelling	Direct	Direct and tunnelling	Observed
400	7.7 (− 20)[a]	4.3 (− 17)	2.0 (− 21)	1.1 (− 20)	1.5 (− 16)
600	9.8 (− 17)	6.3 (− 16)	1.1 (− 17)	2.1 (− 17)	1.1 (− 15)
1000	3.2 (− 14)	5.6 (− 14)	1.3 (− 14)	1.6 (− 14)	4.9 (− 14)
1500	6.8 (− 13)	8.7 (− 13)	5.4 (− 13)	6.0 (− 13)	1.2 (− 12)[b]
2000	3.4 (− 12)	3.9 (− 12)	3.9 (− 12)	4.1 (− 12)	5.9 (− 12)[b]

[a] Should be read as 7.7×10^{-20} cm^3 molecule^{-1} s^{-1}.
[b] Extrapolated from fit to present data.

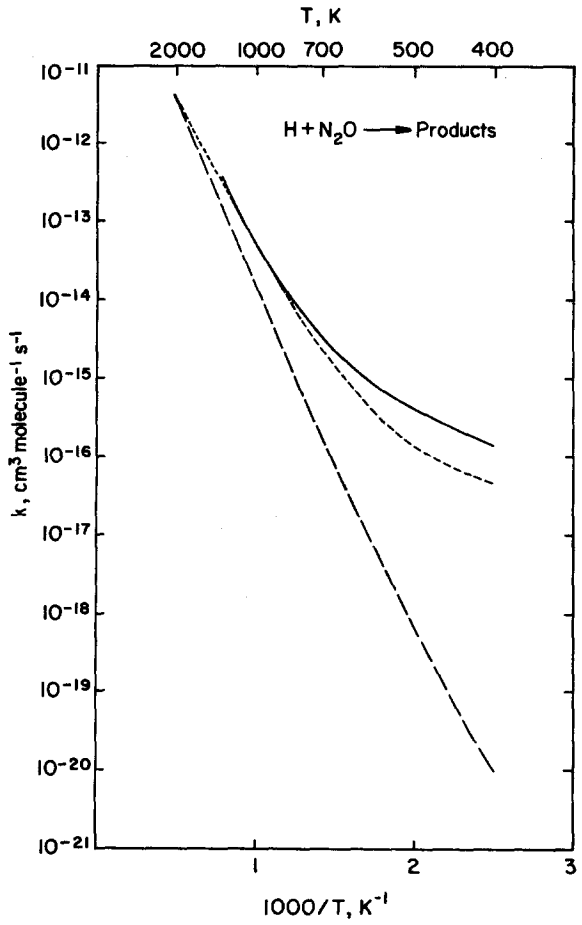

FIG. 4. Comparison of experimental results for $H + N_2O \rightarrow OH$ with predicted values from BAC-MP4 data combined with tunneling through an Eckart barrier. This work (—). 1,3-Hydrogen shift model with HNNO intermediate (- - -). Direct model (– –).

While the direct process has a slightly higher activation energy, it also has a slightly greater preexponential factor than the indirect process. Thus, the direct process could become the dominant pathway for $T \gtrsim 2000$ K. (The relative importance of these two competing pathways is sensitive to the accuracy on the BAC-MP4 barrier heights.) At the lower temperatures ($T \lesssim 750$ K), on the other hand, the indirect or hydrogen shift model performs dramatically better. This comes about because of the much greater influence of tunneling on the intramolecular hydrogen transfer. The impressive agreement with Eq. (6) shown in Fig. 4 strongly supports the hydrogen shift mechanism; the discrepancy at 400 K corresponds to errors of either 5 kJ mol^{-1} in the barrier height or 5% in the imaginary frequency, both well within BAC-MP4 uncertainties. This dramatic effect of tunneling is due to the stable intermediate precursor to the 1,3-hydrogen shift transition state giving rise to a large internal barrier of 131 kJ mol^{-1} relative to the HNNO well compared to the overall barrier height of only 65 kJ mol^{-1} relative to $N_2O + H$. The net result is a large imaginary frequency. In fact, the simple one-dimensional treatment underestimates the actual tunneling probability. However, our treatment is adequate within the accuracy of the barrier heights and frequencies from the BAC-MP4 method.

B. A potential recombination channel

A possible alternative cause for the curvature in Fig. 1 which needs to be addressed is stabilization of the HNNO adduct (Fig. 3):

$$H + N_2O \underset{k_b}{\overset{k_f}{\rightleftharpoons}} HNNO^* \xrightarrow{\beta k_s[M]} HNNO. \qquad (1c)$$

In view of the observed pressure independence (down to $[M] \approx 10^{18}$ cm^{-3}) this process is unlikely. However, we cannot exclude the possibility of reaction (1c) being at its high-pressure limit and therefore analyze it in more detail, thermodynamically and kinetically. $\Delta G^\circ_{f,400\,K}$(HNNO) ≈ -35 kJ mol^{-1}, implying $K_{eq} = 1.9 \times 10^{-15}$ for $H + N_2O \rightleftharpoons HNNO$ in molecule cm^{-3} units. Even with an initial low $[N_2O]$ of 10^{16} cm^{-3} (Table I), 95% of atomic H would be removed at equilibrium. Reaction (1c) is therefore barely plausible on thermodynamic grounds at the lowest temperatures investigated; at higher temperatures the equilibrium is less favorable and HNNO formation can be neglected.

In order to test the kinetics of (1c) we employ the QRRK model described by Dean.[42] Input parameters for 400 K derived from Table IV are $k_f = 1.0 \times 10^{-12}$ cm^3 $molecule^{-1}$ s^{-1}, a preexponential factor for k_b of 1.7×10^{13} s^{-1} and the critical energy for the decomposition of HNNO of 77 kJ mol^{-1}. BAC-MP4 yields a geometric mean frequency for HNNO of 1084 cm^{-1}. Reasonable values for the Lennard-Jones collision rate k_s with M and the collisional deactivation efficiency β of 8×10^{-10} cm^3 $molecule^{-1}$ s^{-1} and 0.25 are assumed.[43] For (1c) QRRK predicts apparent bimolecular removal rate coefficients for H of 9.5×10^{-15} and 3.7×10^{-14} cm^3 $molecule^{-1}$ s^{-1} at 80 and 320 Torr, respectively. This would suggest that the reaction is in the third-order regime, in disagreement with the observed pressure independence. Thus, reaction (1c) is ruled out as a major pathway.

C. Minor reaction channels

1. Estimates of k for $H + N_2O \rightarrow NH + NO$ (1b)

Anderson *et al.*[22] have given evidence that this minor pathway is the source of NH observed in H_2/N_2O and CH_4/N_2O flames at $T \gtrsim 2000$ K, and Baldwin *et al.*[23] considered this channel to be responsible for the NO they found in their CSTR. Before discussing the few measurements of k_{1b} we consider the relevant thermochemistry to arrive at an upper limit for this rate coefficient.

ΔH°_f of NH has been a matter of some disagreement, which has presumably been the reason for the wide variation in quoted estimates of $\Delta H^\circ_{298\,K}$ for process (1b) which range from[44] 92 to 173 kJ mol^{-1}.[17] Recent work gives $\Delta H^\circ_{f,0\,K}$ for NH as 356.5 ± 1.7 kJ mol^{-1},[45] and a review concludes that the value is 356.1 ± 1.3 kJ mol^{-1}.[46] This is consistent with the BAC-MP4 value of 366 kJ mol^{-1}.[35] A value of 356 kJ mol^{-1} is employed here, leading[38] to $\Delta H^\circ_{0\,K} = 145$ kJ mol^{-1} for reaction (1b). We estimate $\Delta H^\circ_{298\,K} = 147$, $\Delta H^\circ_{1000\,K} = 141$, and $\Delta H^\circ_{2000\,K} = 132$ kJ mol^{-1}. Combined with data for H, N_2O, and NO[38] K_{eq} for reaction (1b) is calculated to be $420 \exp(-17\,340\ K/T)$, which is similar

TABLE VI. Literature rate coefficient measurements on $H + N_2O \rightarrow NH + NO$, expressed in the form $k_{1b}(T) = A \exp(-B/T)$.

A (cm^3 $molecule^{-1}$ s^{-1})	B (K)	T range (K)	Comments
6.3×10^{-10}	17 360	1650–1950	Ref. 21 flame study
1.0×10^{-9}	14 600	850–2000	Ref. 44 shock tube and CSTR
8.6×10^{-17}	···	873	Ref. 23 CSTR
3.2×10^{-10}	17 360	1600–2100	Ref. 32 shock tube
8.5×10^{-10}	16 380	670–1840	Ref. 47 flame study[a]
5.4×10^{-8}	32 140	1760–2850	Ref. 48 shock tube[a]
1.8×10^{-13}	···	1790	Ref. 49 upper limit from flame study

[a] Calculated here from the reverse reaction as described in the text.

to $K_{eq} = 180 \exp(-17590\ K/T)$ implicitly used by Hanson and Salimian.[16] Using an activation energy equal to the endothermicity and a generous preexponential factor of 1×10^{-9} cm^3 $molecule^{-1}$ s^{-1} an upper limit to k_{1b} for the region $T \approx 2000$ K is set by

$$k_{1b} \lesssim 1\times10^{-9} \exp(-15800\ K/T)\ cm^3\ molecule^{-1}\ s^{-1}. \quad (7)$$

At lower temperatures an even higher activation energy would be expected because of the increased $\Delta H°$ for reaction (1b), so Eq. (7) is definitely an upper bound for $T \lesssim 2000$ K.

Various determinations of k_{1b} are listed in Table VI. These include two derived from the reverse reaction using K_{eq}, based on the assumption that the major products of the reaction of NH with NO are indeed H and N_2O.[35] These results are plotted in Fig. 5 together with the limit of Eq. (7). Inspection of this figure indicates that of the estimates of k_{1b} in Table VI, those derived from the data of Cattolica *et al.*,[21] Nip,[32] Peterson,[47] and Roose *et al.*[48] lie below the upper limit and hence are compatible with the above arguments. Morley's limit determination[49] is comparable to that given by Eq. (7), $k_{1b} \lesssim 1.5\times10^{-13}$ cm^3 $molecule^{-1}$ s^{-1}. However, two of these estimates lead to inconsistencies. The shock tube

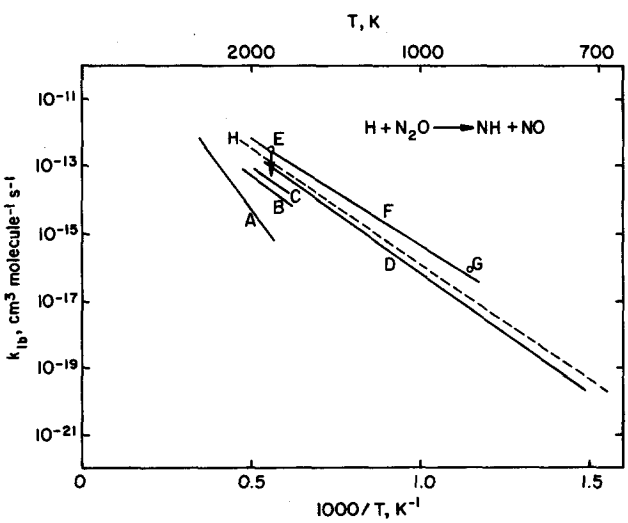

FIG. 5. Comparison of various estimates of $k_{1b}(T)$ for the reaction $H + N_2O \rightarrow NH + NO$. A: Roose *et al.* (Ref. 48), B: Nip (Ref. 32), C: Cattolica *et al.* (Ref. 21), D: Peterson (Ref. 47), E: Morley (Ref. 49) (upper limit), F: Borisov *et al.* (Ref. 44), G: Baldwin *et al.* (Ref. 23), and H: this work (upper limit).

measurements of Nip are derived from determinations of the quantities $k_{1a} + k_{1b}$ and k_{1b}/k_{1a},[32] and his values of k_{1a} show poor agreement with other work. The Arrhenius parameters for k_{1b} of Roose *et al.*,[48] as calculated in this work, imply an unrealistically large preexponential factor (see Table VI).

Of the experiments which fall above our upper limit, those of Borisov *et al.*[44] appear to overestimate k_{1b}, and show an activation energy 11 kJ lower than the newer determinations of the endothermicity. Similarly the value of Baldwin *et al.*[23] is an order of magnitude too high: using $\Delta H°_{1000\,K}$ and the preexponential factor of Eq. (8) we estimate $k_{1b} \lesssim 4\times10^{-18}$ cm^3 $molecule^{-1}$ s^{-1} at 873 K. They calculated k_{1b} from the growth of NO over long time scales, of the order of 100 to 1000 s, and it is possible that reactions not included in the modeling scheme, such as the slow process $N_2O + O \rightarrow 2\ NO$, were significant.

Additionally, the rate of removal of NH by NO has been measured three times at room temperature[50–52] and once[53] from 300 to 380 K. The latter determination showed no temperature dependence. The rate coefficients obtained are in the range 3.8×10^{-11} to 4.7×10^{-11} cm^3 $molecule^{-1}$ s^{-1}. These measurements have not been included in Table VI since, on the assumption that H and N_2O are the reaction products, these rates would imply k_{1b} (298 K) $\approx 1\times10^{-33}$ cm^{-3} $molecule^{-1}$ s^{-1}, which is incompatible with the upper limit for k_{1b} of 2×10^{-35} cm^3 $molecule^{-1}$ s^{-1} based on the above $\Delta H°_{298\,K}$ for reaction (1b). Melius and Binkley have argued that at low temperatures the reaction $NH + NO \rightarrow HNNO$ can occur with no activation barrier.[35] Hence, it may be that at room temperature the reverse of reaction (1b) is not the dominant channel, in accord with the suggestions of Phillips and co-workers.[53]

2. The branching ratio $\alpha = k_{1b}/k_1$

The magnitude of the branching of product channels based on the above discussion can be compared with measurements at various temperatures. Combining Eq. (7) with Eq. 4 for $T \lesssim 2000$ K yields $\alpha \lesssim 1.4 \exp(-5900\ K/T)$, implying $\alpha \lesssim 0.07$ at 2000 K. This is consistent with $\alpha \approx 0.04$ at this temperature derived from the data of Cattolica *et al.*[21] Coupling their[21] value for k_{1b} with an extrapolation of our fit to experimental data, Eq. (6), would give $\alpha \approx 0.02$. At $T \lesssim 1000$ K the limit for the branching ratio can be reduced

by employing the greater endothermicity applicable here to yield $\alpha \lesssim 1.4 \exp(-7000\ K/T)$ which corresponds to $\alpha \lesssim 5 \times 10^{-4}$ at 873 K. In accord with this small α NO was not detected by Albers *et al.* over the range 720 to 1110 K, although they quoted no sensitivity limit.[17]

Golden and Larson[54] have discussed the branching ratio α in terms of the same HNNO intermediate as postulated by Melius and Binkley.[35] This is plausible, since for reaction (1b) reactants and products also correlate on a $^2A'$ surface, cf. reaction (1a). However, they adjusted their model to fit $\alpha(873\ K) = 4 \times 10^{-3}$ from Baldwin *et al.*[23] which appears an order of magnitude too big, from the above. Golden and Larson[54] do not quote any predicted rate coefficients or Arrhenius parameters for k_{1b} and it is unclear whether their modeling would yield the fairly high preexponential factors of Table VI.

3. The $H + N_2O \rightarrow NNH + O$ channel

Figure 3 shows a highly endothermic product channel leading to NNH + O, with predicted $\Delta H^\circ_{300\ K} \approx 203$ kJ mol^{-1}.[35] Using arguments similar to those in the previous section we estimate the branching ratio for this channel to be less than 10^{-3} at 2000 K. Accordingly we do not discuss it further here.

VII. CONCLUSION

An isolated elementary reaction measurement technique has been applied to reaction (1) over the 390 to 1310 K temperature range. At temperatures below 750 K pronounced curvature in the Arrhenius plot is apparent. Theortical work rationalizes this behavior in terms of a single mechanism operating over the full temperature range. This mechanism, rearrangement of an HNNO intermediate to yield principally $N_2 + OH$, involves significant quantum-mechanical tunneling at lower temperatures. At higher temperatures the NH + NO product channel could play a role. To obtain the degree of participation of this channel, direct determinations of k_{1b} are clearly required and these pose a considerable experimental challenge. Not only is the branching ratio small (less than 0.07 at 2000 K), as deduced here from the thermochemistry, but the products NH and NO are likely to undergo further rapid reaction with N_2O and H.

ACKNOWLEDGMENTS

The Rensselaer work was supported by the U. S. Army Research Office and the BAC-MP4 Sandia work by the U. S. Department of Energy, Office of Basic Energy Sciences. We are grateful to W. F. Flaherty, D. F. Rogowski, and T. P. Hanna for technical assistance and advice. Thanks are due to Professor R. R. Reeves for the mass-spectrometric analysis of a sample of N_2O.

[1] G. Dixon-Lewis and D. J. Williams, in *Gas-Phase Combustion, Comprehensive Chemical Kinetics*, edited by C. H. Bamford and C. F. H. Tipper (Elsevier, Amsterdam, 1977), Vol. 17, pp. 158–165.
[2] H. W. Melville, Proc. R. Soc. London, Ser A **142**, 524 (1933).
[3] H. W. Melville, Proc. R. Soc. London Ser. A **146**, 737 (1934).
[4] A. M. Dean, D. C. Steiner, and E. E. Wang, Combust. Flame **32**, 73 (1978).
[5] A. M. Dean, R. L. Johnson, and D. C. Steiner, Combust. Flame **37**, 41 (1980).
[6] H. Henrici and S. H. Bauer, J. Chem. Phys. **50**, 1333 (1969).
[7] R. I. Soloukhin, in *14th Symposium (International) on Combustion* (The Combustion Institute, Pittsburgh, 1973), p. 77.
[8] Y. Hidaka, H. Takuma, and M. Suga, Bull. Chem. Soc. Jpn. **58**, 2911 (1985).
[9] G. P. Glass and R. B. Quy, J. Phys. Chem. **83**, 30 (1979).
[10] G. P. Fenimore and G. W. Jones, J. Phys. Chem. **63**, 1154 (1959).
[11] G. Dixon-Lewis, M. M. Sutton, and A. Williams, J. Chem. Soc. **1965**, 5724.
[12] G. Dixon-Lewis, M. M. Sutton, and A. Williams, in *10th Symposium (International) on Combustion* (The Combustion Institute, Pittsburgh, 1965), p. 495.
[13] V. P. Balakhnine, J. Vandooren, and P. J. Van Tiggelen, Combust. Flame **28**, 165 (1977).
[14] R. R. Baldwin, A. Gethin, and R. W. Walker, J. Chem. Soc. Faraday Trans. 1 **69**, 352 (1973).
[15] D. L. Baulch, D. D. Drysdale, and D. G. Horne, *Evaluated Kinetic Data for High Temperature Reactions* (Butterworths, London, 1973), Vol. 2, p. 453.
[16] R. K. Hanson and S. Salimian, in *Combustion Chemistry*, edited by W. C. Gardiner, Jr. (Springer, New York, 1984), pp. 400–404.
[17] E. A. Albers, K. Hoyermann, H. Schacke, K. J. Schmatjko, H. Gg. Wagner, and J. Wolfrum, *15th Symposium (International) on Combustion* (The Combustion Institute, Pittsburgh, 1975), p. 765.
[18] K. E. Shuler, J. Chem. Phys. **21**, 624 (1953).
[19] R. J. Donovan and D. Husain, Chem. Rev. **70**, 489 (1970).
[20] D. Husain, Ber. Bunsenges. Phys. Chem. **81**, 168 (1977).
[21] R. J. Cattolica, M. D. Smooke, and A. M. Dean, Sandia Report SAND82-8776; presented at Western States Section, The Combustion Institute, Fall Meeting 1982, Livermore, California, October 11–12, 1982.
[22] W. R. Anderson, L. J. Decker, and A. J. Kotlar, Combust. Flame **48**, 179 (1982).
[23] R. R. Baldwin, A. Gethin, J. Plaistowe, and R. W. Walker, J. Chem. Soc. Faraday Trans. 1 **71**, 1265 (1975).
[24] P. Marshall and A. Fontijn, J. Chem. Phys. **85**, 2637 (1986).
[25] K. Mahmud, P. Marshall, and A. Fontijn, J. Phys. Chem. **91**, 1568 (1987).
[26] W. Felder, A. Fontijn, H. N. Volltrauer, and D. R. Voorhees, Rev. Sci. Instrum. **51**, 195 (1980).
[27] W. Felder and A. Fontijn, Chem. Phys. Lett. **67**, 53 (1979).
[28] H. Okabe, *Photochemistry of Small Molecules* (Wiley, New York, 1978), pp. 219–226.
[29] P. Marshall, Comput. Chem. (in press).
[30] P. R. Bevington, *Data Reduction and Error Analysis for the Physical Sciences* (McGraw-Hill, New York, 1969), p. 242.
[31] W. E. Wentworth, J. Chem. Ed. **42**, 96 (1965).
[32] Nip. W. Ph.D. thesis, University of Toronto, 1974, as quoted in Ref. 16.
[33] G. R. A. Johnson and M. Simic, J. Phys. Chem. **71**, 1118 (1967), as calculated in Ref. 14.
[34] M. Schiavello and G. G. Volpi, J. Chem. Phys. **37**, 1510 (1962).
[35] C. F. Melius and J. S. Binkley, *20th Symposium (International) on Combustion* (The Combustion Institute, Pittsburgh, 1984), p. 575.
[36] C. F. Melius and J. S. Binkley, in *The Chemistry of Combustion Processes*, ACS Symp. Ser. 249, edited by T. M. Sloane (American Chemistry Society, Washington, D. C., 1984), p. 103.
[37] P. Ho, M. E. Coltrin, J. S. Binkley, and C. F. Melius, J. Am. Chem. Soc. **89**, 4647 (1985).
[38] *JANAF Tables* (Dow Chemical Co.). Frequently updated.
[39] D. M. Golden, J. Phys. Chem. **83**, 108 (1979). As pointed out in this reference the analysis is valid only where stabilization of the intermediate is negligible, as is the case here, cf. Sec. VI B.
[40] C. Eckart, Phys. Rev. **35**, 1303 (1930).
[41] H. S. Johnston, *Gas Phase Reaction Rate Theory* (Ronald, New York, 1966), Chap. 2. There is a typographical error in its Eq. (2-22): the $2\pi^2/16$ term should be $4\pi^2/16$.
[42] A. M. Dean, J. Phys. Chem. **89**, 4600 (1985).
[43] W. C. Gardiner, Jr. and J. Troe, in *Combustion Chemistry*, edited by W. C. Gardiner, Jr. (Springer, New York, 1984), p. 187.
[44] A. A. Borisov, V. M. Zamanskii, and G. I. Skachkov, Kinet. Katal. **19**, 38 (1978).

[45]S. T. Gibson, J. P. Greene, and J. Berkowitz, J. Chem. Phys. **83**, 4319 (1985).
[46]W. R. Anderson (to be published).
[47]R. C. Peterson, Ph.D. thesis, Purdue University, West Lafayette, Indiana, 1981, as quoted in Ref. 16.
[48]T. R. Roose, R. K. Hanson, and C. H. Kruger, *18th Symposium (International) on Combustion* (The Combustion Institute, Pittsburgh, 1981), p. 53.
[49]C. Morley, *18th Symposium (International) on Combustion* (The Combustion Institute, Pittsburgh, 1981), p. 23.
[50]S. Gordon, W. Mulac, and P. Nangia, J. Phys. Chem. **75**, 2087 (1971).
[51]I. Hansen, K. Hoinghaus, C. Zetsch, and F. Stuhl, Chem. Phys. Lett. **42**, 370 (1976).
[52]J. W. Cox, H. H. Nelson, and J. R. McDonald, Chem. Phys. **96**, 175 (1985).
[53]J. A. Harrison, A. R. Whyte, and L. F. Phillips, Chem. Phys. Lett. **129**, 346 (1986).
[54]D. M. Golden and C. W. Larson, *20th Symposium (International) on Combustion* (The Combustion Institute, Pittsburgh, 1984), p. 595.